

Development and physiological assessments of multimedia avian esophageal catheter system

Kaoru Nakada^{1*}, Jun-ichi Hata²

Abstract

We developed multimedia esophageal catheters for use with birds to measure and record ECG and angular velocity while anesthetized, at rest, and in flight. These catheters enable estimates of blood pressure based on readings given by an angular velocity sensor and by RR intervals of ECG affected by EMG. In our experiments, the catheters had the following characteristics: 1. Esophageal catheters offer a topological advantage with 8-dB SNR improvement due to elimination of electromyography (EMG). 2. We observed a very strong correlation between blood pressure and the angular velocity of esophageal catheter axial rotation. 3. The impulse conduction pathway (Purkinje fibers) of the cardiac ventricle has a direction opposite to that of the mammalian pathway. 4. Sympathetic nerves predominate in flight, and RR interval variations are strongly suppressed. The electrophysiological data obtained by this study provided especially the state of the avian autonomic nervous system activity, so we can suspect individual's health condition. If the change of the RR interval was small, we can perform an isolation or screening from the group that prevent the pandemics of avian influenza. This catheter shall be useful to analysis an avian autonomic system, to perform a screening, and to make a positive policy against the massive infected avian influenza.

Key Words: Angular Velocity Sensor, Autonomic Nerve, Avian Influenza, Screening

I. BACKGROUND

1.1. Objective

Our goal is to screen for birds with avian influenza. To this end, we attached wireless packet transceivers equipped with three-axis angular velocity sensors on the backs of whooper swans (*Cygnus cygnus*), then released the birds into the wild. In the present study, to gather basic data, we developed a multimedia esophageal catheter system equipped with both differential ECG electrodes and the angular velocity sensors incorporated into the transceivers attached to the swans. We used the data gathered with the instrument to perform physiological analyses.

1.2. Physiology of avian influenza infection

In the wild, ducks, geese, and other waterfowl are reservoirs of the Type A influenza virus. Typically, some 30% of the total population are carriers. The virus multiplies in the intestines of waterfowl and is released into water via feces, infecting other waterfowl and perpetuating the infection cycle. Infected waterfowl are asymptomatic. However, the virus mutates at a high rate; after mutating to a strain that is highly toxic to the host, the virus produces symptoms in, and may even lead to the death of the infected waterfowl. According to the World Organization for Animal Health (OIE), highly pathogenic avian influenza is defined by greater than 75% mortality within 10 days of inoculation of at least eight susceptible

four to eight-week-old chicks. Separately, research groups studying influenza at the molecular level report that highly pathogenic viruses feature consecutive basic amino acids at the HA cleavage site. H5 and H7 fall into this category [1,2,3]. According to the OIE definition, viral strains causing 74% mortality are weakly pathogenic, but still kill numerous host creatures. We believe the terms *highly* and *weakly* pathogenic do not correlate well with actual virulence and are without clinical or epidemiological meaning.

In this social context, the International Telecommunications Union (ITU) has called on many countries to draw on information communications technologies (ICT) to boost countermeasures against avian influenza [4-9]. We perceive a need for a sensor system capable of capturing and transmitting avian biological signals; based on this idea, we are pursuing development and verification experiments as part of overall basic research efforts. This report is a part of these efforts.

As a general rule, when virulent viruses multiply in the lungs or digestive tract of birds, inflammation affects the entire body. Histamine and other chemical mediators are released from various inflamed tissue, increasing the permeability of vascular endothelial cells. This results in the excessive consumption of the endogenous epinephrine that elevates blood pressure, shortening RR intervals (ECG R wave intervals), reducing CVRR (standard deviation of RR interval), and weakening the control of sympathetic and parasympathetic nerves. In attempting to screen for avian influenza infections, this means it is

Manuscript received May 05, 2018 ; Accepted May 29, 2018. (ID No. JMIS-2018-0031)

Corresponding Author (*): Kaoru Nakada, Shimokasuya 143, Isehara, Japan. +81-463-913130, tanaka@ets8.jp

¹Tokai University School of Medicine, Isehara, Japan

²Central Institute for Experimental Animals, Kawasaki, Japan, jhata@i.softbank.jp

imperative to monitor not just breathing patterns associated with pneumonia, but the autonomic nerves, including the circulatory system. This report describes a special esophageal catheter incorporated into a multimedia system to gather the circulatory system data and analyze and assess the physiological features.

1.3. Avian physiological characteristics

Birds evolved from theropod dinosaurs during the Jurassic, some 150 to 200 million years ago. Modern birds are believed to be the only dinosaur group to have survived an asteroid impact and the resulting extinction event occurring some 65 million years ago. Birds differ markedly from mammals, in particular humans, in many physiological aspects [10-13].

1.3.1. Respiratory organs

The avian lung is hard and hardly expands or contracts. Birds lack diaphragms and breath by sending air to the lung from the trachea and air sacs, which function as bellows []. Thoracic and abdominal skeletal muscles allow air sacs to expand and contract. This means ECG measurements at the thoracic wall are impacted by EMG signals originating from these muscles.

1.3.2. Circulatory organs

Under an electron microscope, we observe in birds the transverse tubes around the Z line, which involve in calcium metabolism in mammals and reptiles, but not in the left ventricular myocardial cells. Thin myocardial fibers polymerize to form thick fibers. Even in normal avian hearts, cross sections of avian myocardial fibers appear histopathologically to indicate diastolic myocarditis. The ejection fraction (amount of blood remaining in the left ventricle) for humans is about 50%; for birds, the figure is close to 1%. Virtually no blood remains in the left ventricle. With each beat, virtually all blood in the heart is expelled into a major vessel.

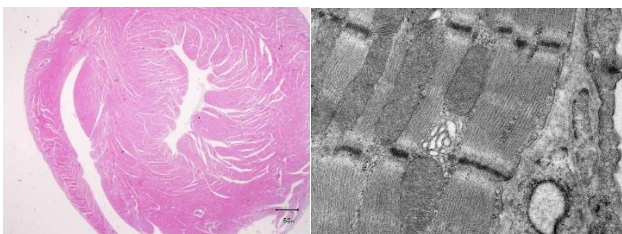


Fig. 1. Left: Cross-section of heart. Normal heart appearing to indicate diastolic myocarditis. Right: Electron microscopic image of the left ventricle. No transverse tube near Z line (chicken).

As for the histology of impulse conducting system, while, in mammals, the His bundle runs downward from the AV node along the interventricular septum, in birds, the His bundle issues from the cardiac wall and runs downward in the subepicardial region. Avian Purkinje fibers run from

the subepicardial to myocardial regions and, ultimately, the endocardium [09]. The major vessel in birds is right descending aorta, while the major vessel in mammals is the left descending aorta. Therefore in the present article, negative QRS waves are described as R waves and not as Q or S waves.

1.3.3. Crop and esophagus

Many birds have a crop in the lower esophagus, comparable to a diverticulum. However, crows lack this crop. This allows us to insert an esophageal catheter in a blind manner with no special equipment. In humans, the thoracic esophagus runs next to the posterior mediastinum; in birds, the esophagus runs next to the left atria. This means that vibrations generated by cardiac pulsation have significant impact on esophageal catheters Figure. 2.

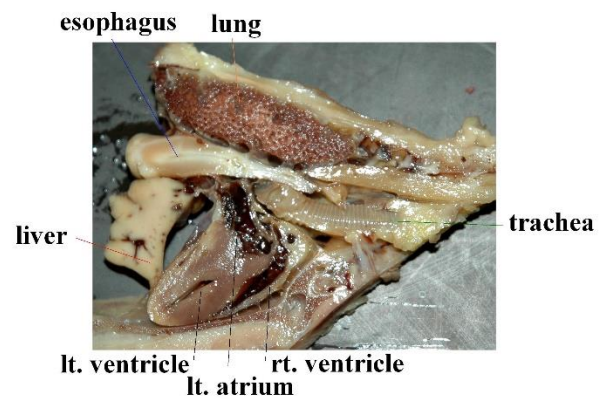
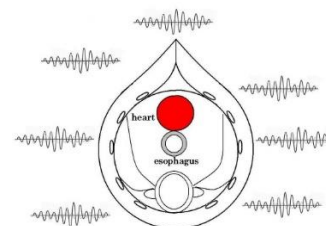


Fig. 2. Positional relationship between heart and esophagus. The left atrium is next to the esophagus.

II. PRINCEPLE

2.1. Topological noise reduction effects

In birds, the thoracic and abdominal skeletal muscles act as a diaphragm to control the air sacs. Breathing is generally involuntary, but can be controlled voluntarily when needed. In most cases, the skeletal muscles are believed to be controlled by the brainstem. At the center of the thoracic cavity, the EMG values anticipated are near zero because the EMG from skeletal muscles is circumferential (0 to 360 degrees). When performing ECG in the esophagus, we can have a benefit of noise reduction due to its topological position.



Expected noise values from 0 to 360 degrees = 0

Fig. 3. Topological noise reduction effects

2.2. Angular velocity sensor

In birds, the esophagus runs adjacent to the left atrium. This means the vibrations of cardiac pulsation have significant impact on an esophageal catheter. For this reason, we performed measurements using an angular velocity sensor. The physical and electrical properties of the sensor are given below.

The piezoelectric strain constant, $d_{31}(m/V)$, represents the scale of strain resulting from applying electric voltage without stress.

$$d = K \cdot \epsilon T \cdot sE \dots\dots\dots(1)$$

where K is the electromechanical coupling coefficient, ϵT the dielectric constant, and sE the compliance.

The piezoelectric output constant, $g_{31}(v.m/N)$, represents the scale of electric voltage resulting from applying stress without electrical displacement.

$$g = d / \epsilon T \dots\dots\dots(2)$$

where d is piezoelectric constant and ϵT the dielectric constant.

Additionally, d_{31} and g_{31} represent one of the 3-axis modes.

Output voltage, V , in relation to external force, F

$$V = (3/8) \cdot g_{31} \cdot (L/t \cdot w) \cdot F \dots\dots\dots(3)$$

where L is the length of the element, t the thickness of the element, and w the width of the element.

Defining F_c as the Coriolis force, m vibrator mass, and f resonant frequency of the element, we obtain the following formula:

$$F_c = m \cdot (V \cdot 2\pi f) \dots\dots\dots(4)$$

The Coriolis force generated inside the applied external force entails hysteresis but a linear relationship applies overall. Our study used the following formula:

$$F_c = a \cdot F \dots\dots\dots(5)$$

Using a Murata ENC-03RC and with V representing the generated electric potential and actual angular velocity given in degrees/sec, we arrive at the following:

$$V = 0.67 \cdot \text{degree mV/sec. } f = 32 \text{ kHz}$$

Hence the external force impacting the sensor is:

$$F = (2 \cdot E + 6) \cdot (1/a) \cdot m \cdot \text{degree}$$

Since m is a mass constant and hysteresis is averaged, the external force applied and rotating angular velocity form a linear direct function. Figure 4 shows the Murata angular velocity sensor. Figure 5 illustrates the angular velocity of axial rotation within the esophageal catheter [14-17].

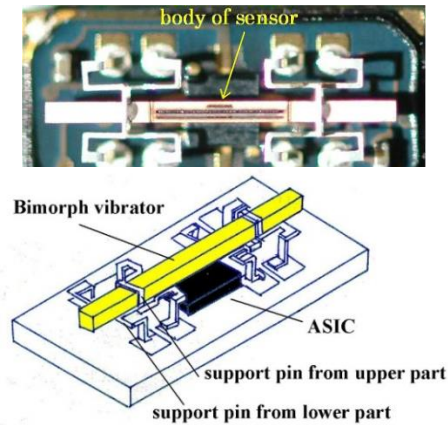


Fig. 4. Internal structure and illustration of angular velocity sensor (ENC-03RC)

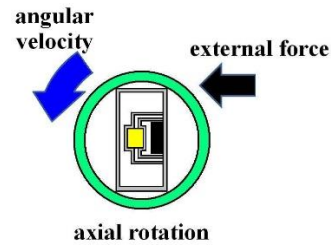


Fig. 5. External forces can be calculated by measuring the angular velocity of the rotation.

III. METHODS

3.1. Developed equipment

Figure 6 shows our data logger and esophageal catheter. Tables 1 and 2 summarize their specifications. Figure 7 is a block diagram of the data logger. We secured the angular velocity sensor of the esophageal catheter by applying an adhesive to the tip and at 60 mm from the oral-side end. The differential ECG electrodes were 10 mm in width and were positioned 10 mm apart to ascertain catheter depth based on ECG waveforms. These +1 and +2 electrodes were designed mainly to measure the ventricle and atrium, respectively. For the angular velocity sensor, a reference sensor was implanted 60 mm from the oral-side end to eliminate the effects of up and down movements during flight and isolate cardiac beats (Figure 8).

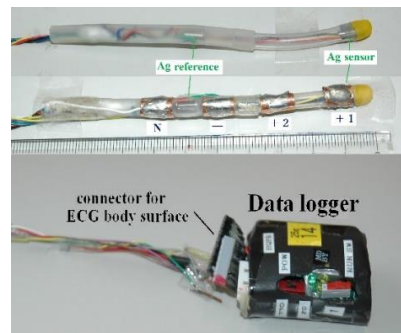


Fig. 6. Data logger and esophageal catheter (two-channel bipolar ECG, differential angular velocity sensor)

Table. 1. Catheter specifications

	Differential ECG	Angular velocity	Tube shape
Model 2 (for flight)	Two-channel bipolar ECG Electrode width: 10 mm Electrode interval: 10 mm	Two sensors (differential) A reference was added to 60 mm from the oral end	Internal diameter: 3 mm External diameter: 5 mm Made of silicone

Table. 2. Data logger specifications

CPU	A/D channel count	A/D conversion	Amplifier circuit AD623	Battery	Total weight
ARM LPC1768	7 channels	Potential axis : 16 bits, Time axes: 1 kHz, 2 kHz, 5 kHz	ECG: x100 Angular velocity : x10	3.7 V (2 g)	32 g

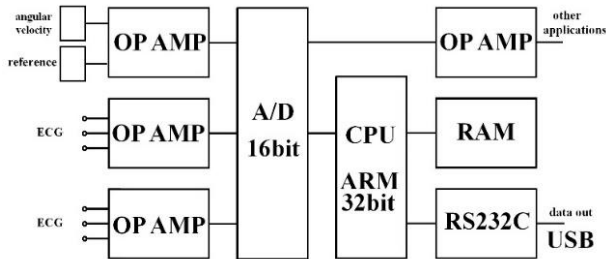


Fig. 7. Block diagram of data logger (three other channels for A/D input omitted)

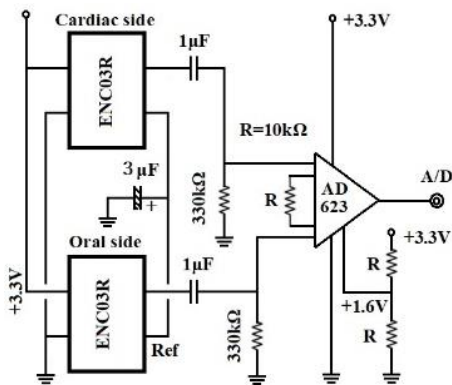


Fig. 8. Circuit diagram of differential angular velocity amplification (the lower sensor is the reference sensor)

3.2. Experiment procedures

Figure 9 is a schematic diagram of the study setup. With chickens, we induced inhalation anesthesia (average 2.5%) with isoflurane for continuous direct blood pressure monitoring on the axillary artery. With carrion crows allowed to fly outdoors, we administered local anesthesia to attach the electrodes; we administered 1.5% isoflurane by inhalation to induce mild sedation when inserting esophageal catheters. Once fully roused, these crows were held in our hands and carried outside, then released to move and fly within a large netted cage (a tennis court). The sampling of all analog-digital conversion was set to 1,000/sec for crows and to 2,000 or 5,000/sec for chickens. Lattices were recorded in 16 bits.

3.3. Subjects

The chickens used were purchased from a laboratory animal vendor. Feral crows trapped by a local government agency were obtained legally. The pigeons were donated pedigreed racing pigeons that competed in the Wakkanai 1,000 km (grand national race).

Table. 3. Study subjects

	number	gender	body weight	remarks
Hens	32	female	560 – 1290 g	breed free of arrhythmia
Carrion crows (<i>Corvus corone</i>)	28	unknown	330 – 650 g	Tsuruoka city
Jungle crows (<i>Corvus macrorhynchos</i>)	18	unknown	420 – 890 g	Tsuruoka city, Hiratsuka city
Pigeons	9	unknown	400 – 520 g	Yamazaki Kiyoshi Pigeons

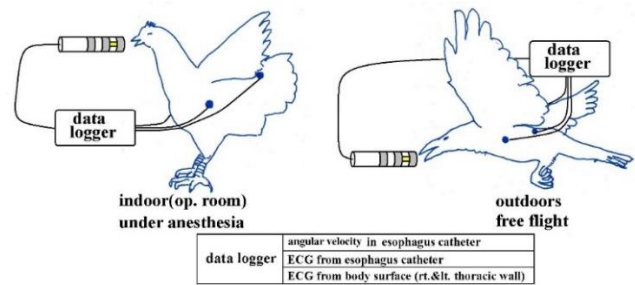


Fig. 9. Study concept and electrode placement

3.3.1. Comparison of esophageal catheter and thoracic wall ECGs

Using seven carrion crows, we compared esophageal catheter ECG and thoracic wall ECG to ascertain the noise reducing effects of the esophagus on EMG.

3.3.2. Correlation between blood pressure and esophageal catheter angular velocity

Unanesthetized carrion crows were placed in an outdoor netted cage (a covered tennis court). We measured angular velocity and RR intervals with the crows resting, in flight, and walking about [18-20]. Catheters were implanted into chickens after placing them into a supine position under isoflurane inhalation anesthesia (spontaneous respiration). To induce nerve control, we intravenously administered epinephrine (sympathomimetic agent), Inderal (propranolol hydrochloride: sympathetic blocking agent) and atropine (parasympathetic inhibiting and antimuscarinic agent) at doses twice those recommended for adult humans for unit of body weight. With the chickens, we severed the axillary artery and directly inserted a narrow P10 catheter into the artery for continuous monitoring of arterial blood pressure. At the same time, we measured and recorded angular velocity using the esophageal catheter to assess the correlation between angular velocity and blood pressure.

3.3.3. Correlation between catheter depth and angular velocity

Unanesthetized carrion crows were placed in an outdoor netted cage (a covered tennis court) and monitored while resting, during flight, and while walking about. Catheters were implanted into chickens after placing them into a

supine position under isoflurane inhalation anesthesia (spontaneous respiration). We varied catheter depths to analyze the correlation of catheter placement with ECG waveforms and angular velocity.

3.4. Results

3.4.1. Comparison of signal-to-noise ratios between esophageal catheter and thoracic wall ECGs

Figure 10 compares signals obtained with the thoracic wall ECG (electrodes on the left and right thoracic walls, neutral electrode on the back) and the esophageal catheter ECG (electrodes inside the esophagus). Birds lack diaphragms and use air sacs like bellows. Since thoracic wall muscles are always in tension to allow control of air sac tension, EMG interfered with thoracic wall ECG. In contrast, the esophageal catheter ECG was largely free of EMG interference. Table 4 summarizes signal-to-noise (S/N) ratios by treating EMG signals as noise. We found a S/N ratio improvement of about 8 dB with the esophageal catheter ECG compared to the thoracic wall ECG.

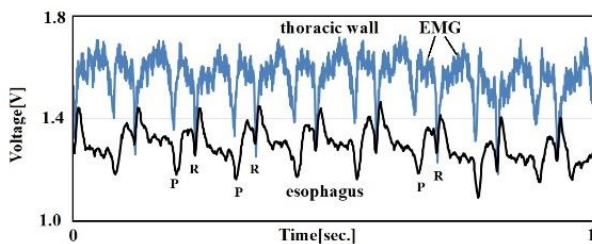


Fig. 10. Comparison between esophageal catheter ECG and thoracic wall ECG (carrion crows)

Table 4. Comparison of S/N between esophageal catheter and thoracic wall ECGs

ID	S/N[dB]							average
	H3	H7	H9	H11	H12	H15	H17	
esophagus	12.0	13.6	11.8	10.9	12.2	10.4	10.2	11.6
battlements	3.6	4.0	3.8	3.3	4.2	2.6	3.8	3.6

3.4.2. Correlation between blood pressure and esophageal catheter angular velocity

After inducing isoflurane anesthesia and with spontaneous respiration, we intravenously administered a pharmaceutical agent (Figure 11: propranolol hydrochloride) to introduce fluctuations in blood pressure; we then measured the angular velocity of the esophageal catheter and direct arterial blood pressure over time. The results demonstrated an extremely high correlation coefficient, R^2 , of 0.93. We carried out the same experiment with ten chickens. Table 5 summarizes the correlation between systolic blood pressure and angular velocity. Comparing the correlation coefficients would be statistically meaningless, since the experiments were undertaken under different conditions, but as a whole, the experiments suggested a strong correlation (average R^2 of 0.95). Cardiac beats as external forces were recorded in

charts that represent the axial rotation of the esophageal catheter.

Figure 12 compares RR intervals calculated from ECG and direct blood pressure (systolic and diastolic blood pressure). Short-cycle variations in the RR interval represented respiratory changes, and large up-and-down changes in the RR interval were synchronous with blood pressure changes. Both are under sympathetic and parasympathetic nerve control. In other words, the results indicate that relative changes in blood pressure can be ascertained by measuring RR intervals.

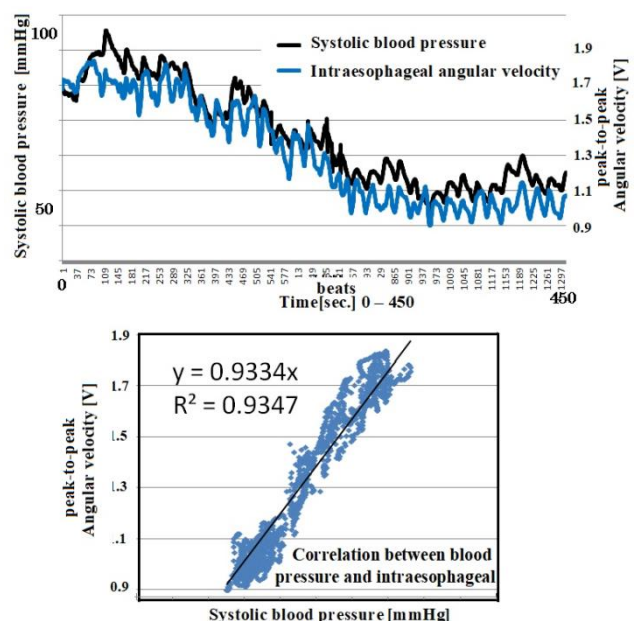
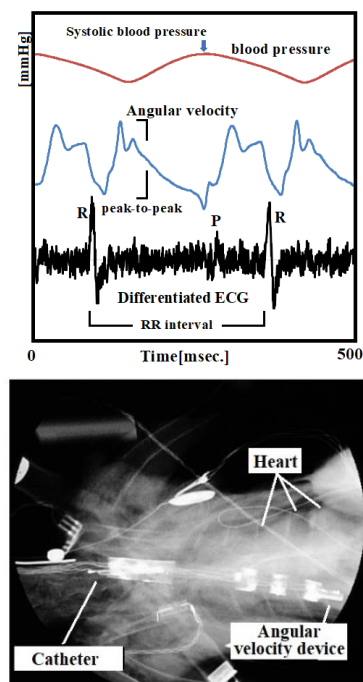


Fig. 11. Correlation between RR intervals and blood pressure (intravenous propranolol hydrochloride)

Table 5. Correlation coefficients between angular velocity and systolic blood pressure for 100 beats (chickens)

ID	N15	N16	N17	N18	N19	N20	N21	N22	N23	N24	Average
Correlation coefficient	0.951	0.977	0.954	0.949	0.939	0.965	0.928	0.966	0.954	0.948	0.953

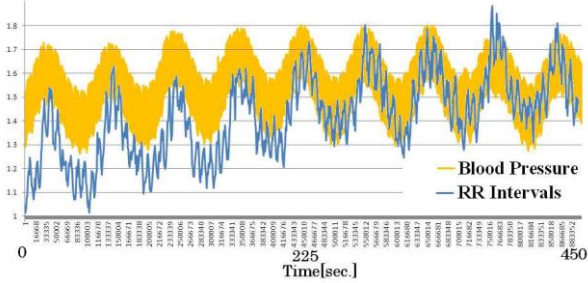


Fig. 12. Changes in direct blood pressure and RR intervals

Moreover, with carrion crows allowed to take flight outside, the results showed that the blood pressure more than doubled from 90 to 210 mmHg before and after flight. During actual flight, CVRR fell to less than 1%, pointing to the predominance of the sympathetic nerves in flight. We observed a strong correlation between blood pressure and RR intervals with resting birds and birds in flight[21].

C. Catheter placement

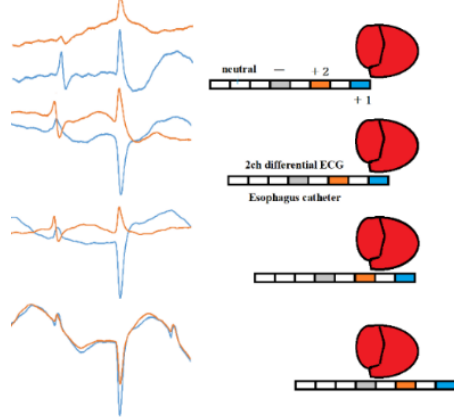


Fig. 13. Differences in ECG relative to catheter depths

Figure 13 shows the differences in ECG relative to the placement of the esophageal catheter (Model 2). The oral-side electrode (“+2” in Figure 13) strongly detected negative bipolar P waves when the electrode was above the atrium. Strong detection of positive bipolar P waves occurred at comparable potentials with the electrode positioned caudal to the atrium. When R waves were positive, the electrode was toward the oral side relative to the ring-shaped coronary artery (between the atrium and ventricle). When R waves were negative, the electrode was caudal to the artery. ST increased when the electrode was implanted caudal to the ring-shaped coronary artery. These findings clearly indicate that ECG can be used to determine the depth of esophageal catheter placement.

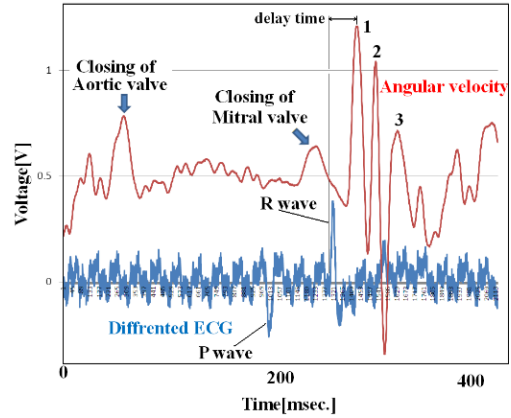
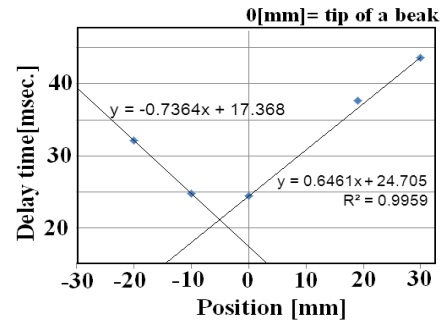


Fig. 14. Relationship between electrode placement and vibration delays associated with cardiac beats

Figure 14 shows the relationship between ECG (one differential to remove direct current components) and angular velocity, indicating the time difference between the start of the R wave and the first peak of angular velocity. ECG data represents electrical movement; the peak angular velocity indicates the maximum axial rotation of the esophageal catheter associated with the force of blood forced out by the pulsing heart. The figure shows that this time delay depends on esophageal catheter placement (average of 100 beats). The reciprocal of the slope of these two lines (average: 1.47 cm/sec) is proportional to the flow rate of blood pumped out to a large vessel by pulsation. If the distance to the axillary artery is 4.5 cm, we would expect the blood to reach the root of the greater pectoral muscle in a little over 3 seconds.



Position[mm]	30	19	0	-10	-20	30
average	46.2	39.9	25.7	26.2	34.0	46.2
distribution	79.0	55.0	68.2	28.0	44.3	79.0
standard deviation	1.53	0.954	3.09	1.05	1.24	1.52

Fig. 15. Relationship between esophageal catheter placement and vibration delays (average of 100 beats)

IV. DISCUSSION

4.1. Investigation on ECG R waves

According to an ornithology textbook by Harrison, the histological impulse conduction pathway of ECG in mammals is that, after the AV node, the His bundle runs downward through the interventricular septum. In birds,

the His bundle issues from the cardiac wall, runs down the subepicardial region, and turns into Purkinje fibers to reach the subepicardial and myocardial regions and ultimately to the endocardium. This suggests that the conduction of the ventricular wall impulse for birds takes the opposite path from that in mammals, generating a force that squeezes from the lateral to medial sides. Figure 13 shows that P and R waveforms vary depending on catheter placement. The patterns of negative R waves for birds were in striking opposition to those in mammals, demonstrating that the impulses are delivered from the surface of the heart toward the endocardia (flow along the Purkinje cells is reversed). To our knowledge, no previous report proves Harrison's electrophysiological ECG impulse conduction system.

4.2. CVRR variations

PR and RR intervals from the standpoint of p waves, RR interval variations can be separated into RP and PR intervals. Figure 16 shows fluctuations in RP intervals, but PR intervals remained stable. The RP interval includes the SA node, while the PR interval includes the AV node. Thus, the SA node involves both sympathetic and parasympathetic nerves, while the AV node involves neither (Figure 17). Visceral vessels are controlled by both sympathetic and parasympathetic nerves. While the peripheral vessels are clearly controlled by sympathetic nerves, whether peripheral vessels are controlled by parasympathetic nerves is unknown [12-15].

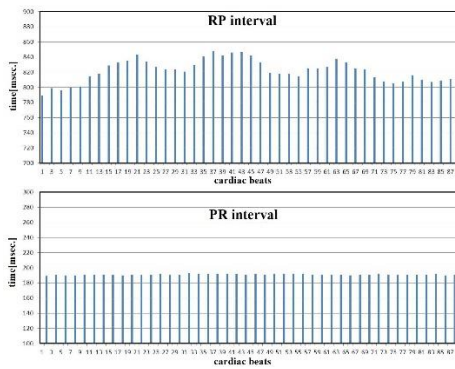


Fig. 16. The RP interval includes SA node. The PR interval includes the AV node

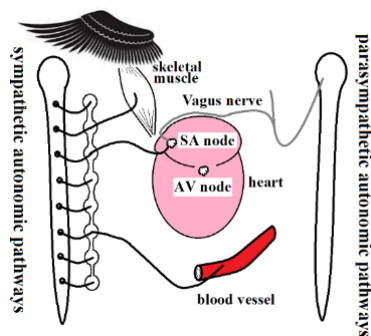


Fig. 17. Estimates of sympathetic and parasympathetic innervation based on electrophysiological data

4.3. Calculating blood pressure in flying carrion crows

We implanted the esophageal catheter in a carrion crow (Figure 18), and then released the bird from our hands, allowing it to flight off. Figure 19 shows the RR intervals before and after flight. High-frequency respiratory variations and autonomic nerve variations were seen before flight; once the crow was in flight, these variations were significantly suppressed ($\leq 1\%$ CVRR). This RR interval control suggests flapping is achieved not only by motor nerves that control skeletal muscles but also by the contraction of vessels in the heart and entire body. In humans, this pattern of sympathetic nerve dominance is comparable to the physiological state generated by a 100-meter sprint. Birds are capable of maintaining this state of sympathetic nerve dominance. For example, the bar-tailed godwit (*Limosa lapponica*) flies 12,000 km nonstop over the course of 13 days from New Zealand to Okinawa. Autonomic nerve control remains functional even when sympathetic nerves are allowed to dominate for 13 days. This suggests that it may be possible to identify sick birds based on failure to achieve sympathetic nerve dominance [22-27].



Fig. 18. After catheter implantation, we released the crows into the enclosure for data gathering.

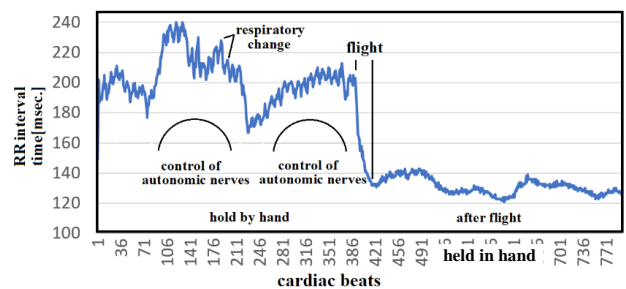


Fig. 19. RR intervals before and after flight

4.4. Application to avian influenza screening

About 20 billion domestic fowls (chickens, quails, ducks, pheasants, etc.) are being raised worldwide, and the size of this market is estimated at 120 billion US dollars per year. The Center for Disease Control in the US investigated past global pandemics and clarified that avian influenza viruses (H1, H2 and H3) directly infected humans without infecting pigs. The previous new influenza virus was a porcine virus, but it did not result in a pandemic, and its mortality was comparable to seasonal influenza viruses. The European Union investigated the issue with a possibility of challenging WHO Secretary General in an international court for issuing a pandemic declaration.

Three main countermeasures for avian influenza employed by the government of Japan (Ministry of Agriculture, Forestry and Fisheries) include: burning and disposing of dead and infected birds, restricting the transfer of domestic fowls from influenza-infected areas and testing, and supporting producers in an event of highly pathogenic avian influenza virus outbreak. There is no proactive measure to screen for latent infections. The government takes action only when domestic fowls die, and there has not been any mention of early screening for avian influenza (Figure 20).

In our research, sympathetic and parasympathetic nerve control could be deduced by measuring RR intervals using an angular velocity sensor. In birds with avian influenza, inflammation causes mast cells to release chemical mediators, such as histamine, to elevate vascular permeability. Since autonomic nerve control is negatively affected from an early stage, the early screening of infected birds may be possible.

At present, the Ministry of Agriculture, Forestry and Fisheries of Japan takes action only when domestic fowls die and retroactively acts to stop transferring or destroying nearby domestic fowls. However if autonomic nerve abnormalities can be detected before the level of antibodies elevates, suspected birds can be isolated early. If infected birds can be isolated early, herd infections can be prevented, and we believe that ICT can be a breakthrough technology for non-contact avian autonomic nerve monitoring.

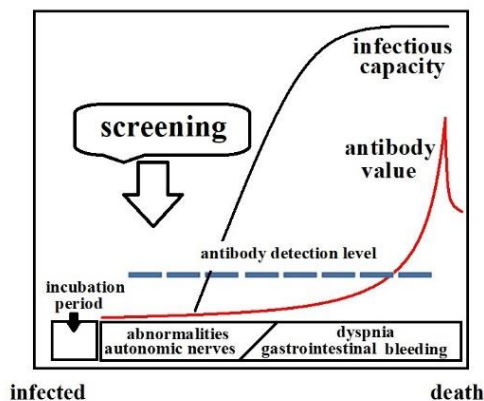


Fig. 20. Conceptual diagram of early screening

V. CONCLUSIONS

We developed esophageal catheters for use with birds to record ECG and esophageal angular velocity as measured during anesthesia, while resting, or in flight. The ECG and angular velocity measurements made with these catheters had the characteristics listed below, suggesting that the catheters would be useful in screening for avian influenza:

1. Esophageal catheters offers topological advantages that eliminate the effects of EMG.
2. A strong correlation exists between blood pressure and angular velocity of the axial rotation of the esophageal catheter.
3. The impulse conduction pathway passing through the ventricle (Purkinje fibers) for birds is opposite to that for mammals.
4. The sympathetic nerves are overwhelmingly predominant for birds in flight, and RR interval variations are strongly suppressed.
5. ICT technology capable of monitoring autonomic nerve activity in birds may be useful in screening for avian influenza.

Acknowledgements

This study was undertaken from 2012 to 2018 after appropriate review and approval by the institutional animal ethics committee at Tokai University.

Our research was funded by grants-in-aid for scientific research (Grants 21241042 and 23651169) from the Ministry of Education, Culture, Sports, Science and Technology. For their contributions to the work described in this paper, we are deeply indebted to all those at Tokai University School of Medicine, in particular Prof. Isao Nakajima, Prof. Yoshiya Muraki, Prof. Toshihiko Kitano, Ms. Noriko Numata, Ms. Miyoshi Tanaka, Ms. Yukie Tanaka, Ms. Katsuko Naito, and Ms. Yoshiko Ito who were helpful at all times and provided essential assistance. We also wish to express our heartfelt thanks to Mr. Kokuryou Mitsuhashi of Seisa University Shonan campus for outstanding field assistance. We are also grateful to the Tsuruoka City Government for providing for this research at no cost feral crows captured by a government agency.

REFERENCES

- [1] OIE, "Highly pathogenic avian influenza" 3 May 2018; <https://www.oie.int/doc/ged/D9311.PDF/>
- [2] WHO, "Updated unified nomenclature system for the highly pathogenic H5N1 avian influenza viruses" 3 May 2018; http://www.who.int/influenza/gisrs_laboratory/h5n1_nomenclature/en/
- [3] WHO "Cumulative number of confirmed human cases of avian influenza A(H5N1) reported to WHO" 3 May, 2018; http://www.who.int/influenza/human_animal_interface/H5N1_cumulative_table_archives/en/
- [4] ITU-D RGQ 14-2/2/079-E, Avian Influenza and expected telecommunication technical development.
- [5] ITU-D RGQ 14-2/2/069-E, Liaison Statement on the role of telecommunication/ICT to be used for an integrated ICT network to monitor the avian influenza.
- [6] ITU-D RGQ 14-2/2/070-E, Note to the Director of BDT, Proposal for an integrated ICT network to monitor the avian influenza.

- [7] Working Parties 7B and 7C, Doc 7B/TEMP/38-7C/TEMP/22, ITU-D RGQ 14-2/071-E, Liaison Statement, Reply to a liaison statement from ITU-D Study group 2 regarding an ITU-D Study Group 2 Question.
- [8] I. Nakajima, T. Kitano, M. Katayama, L. Androuchko, "Expected Communications Technology to Track Avian Influenza and Related the Statement of Appeal by ITU-D SG2 Q14", *Int. J. eHealth & Medical Communications* vol.2, no.4, pp.20-37, 2010.
- [9] I. Nakajima, "Telecommunications for Disaster and Pandemics" www.ituaj.jp/wp-content/uploads/2013/04/nb25-2_web-10_tokai.pdf
- [10] J. Maina, "The Lung-Air Sac System of Birds", Springer Berlin Heidelberg New York, 2005.
- [11] P. Jewett, J. Sommer, aE. Johnson, "Cardiac muscle. Its ultrastructure in the finch and hummingbird with special reference to the sarcoplasmic reticulum" *J. Cell Biol.* Vol. 49, No. 50. 1971.
- [12] P. Jewett, S. Leonard, J. Sommer. "Chicken cardiac muscle. Its elusive extended junctional sarcoplasmic reticulum and sarcoplasmic reticulum fenestrations", *J. Cell Biol.* Vol. 56, No. 595. 1973.
- [13] R. Harrison, "Avian Medicine: Principles and Applications", Chapter 27, Zoological Education Network, July 1994. ISB N-13: 978-0963699602.
- [14] muRata, "Angular Rate Sensor ENC-03R", <https://www.elecrow.com/download/ENC-03.pdf>.
- [15] T. Liu, Y. Inoue, K. Shibata, X.Tang, "A Wearable Inertial Sensor System for Human Motion Analysis", *IEEE Sensors Journal*, vol.16, no. 22, pp. 7821-7834, Nov. 2016.
- [16] T. Fitzgerald, E. Rhee, D. Brooks, J. Triedman. "Estimation of cardiac conduction velocities using small data sets", *Proceedings of the Computers in Cardiology 2001*, Sep. 2001.
- [17] M. Tadi, E. Lehtonen, M. Pankäälä, A. Saraste, T. Vasankari, M. Terás, "Gyrocardiography: A new non-invasive approach in the study of mechanical motions of the heart. Concept, method and initial observations", *Proceedings of the Engineering in Medicine and Biology Society (EMBC), IEEE 38th Annual International Conference of.* Aug. 2016.
- [18] Task Force of the European Society of Cardiology and the North American Society of Pacing and Electrophysiology, "Heart rate variability", *European Heart Journal*, Vol.37,pp.354-381, 1996.
- [19] F. Toyoda, T. Morita, A. Miyazaki, T. Mitsuiye, "ECG and A utonomic Nerves in Chicks", *Jpn, Poult. Sci*, vol.36,pp.260-268, 1999.
- [20] D. Lakens, "Using a Smartphone to Measure Heart Rate Changes during Relived Happiness and Anger," *IEEE Trans. on Affective Computing*, vol.4,no.2, pp.238-241, Apr. 2013, DOI: 1109/T-AFFC.2013.3.
- [21] A. Biewener, "Muscle function in avian flight: achieving power and control," *Philos Trans R Soc Lond B Biol Sci.* 366(1570),pp.1496-1506, 2011.
- [22] "Basic Description of the Argos System", Feb. 2018; [www.webpages.uidaho.edu/wlf314/labs/Argos System Description n.pdf](http://www.webpages.uidaho.edu/wlf314/labs/Argos%20System%20Description.pdf).
- [23] North Star, "Tracking Birds," www.northstarst.com/tracking-birds, Mar. 2018.
- [24] O. Roy, J. Hart, "Transmitter for Telemetry of Biological Data from Birds in Flight", *IEEE Transactions on Bio-medical Electronics*, Vol.10, No.3, pp.114-116, July 1963.
- [25] E. Morishita, K. Itao, K. Sasaki, H. Higuchi, "Movements of Crows in Urban Areas, Based on PHS Tracking"; www.airies.or.jp/attach.php/.../save/0/0/07_2-09.pdf, Feb. 2018.
- [26] Y. Li, Y. Yin, "Bird Objects Detection and Tracking on the Wild Field Circumstance", *Proceedings of IEEE Computer Society WRI World Congress on Computer Science and Information Engineering*, 2009.
- [27] D. Brown, "Birds Fly More Than 7,000 Miles Nonstop, Study Shows", *Washington Post*, October 22, 2008.

Authors



Kaoru Nakada graduated Tokai University School of Medicine in 1980. He had finished his clinical resident course at Toshima Hospital in Tokyo and opened his clinic in Shudama Town Yamanashi Japan 1985. He got the board member of the International Chinese Medicine in 1995. Since 2009, he has been investigated on influence of the sympathetic nervous system of Chinese medicine as a researcher at Nakajima Laboratory of Tokai University Isehara campus. For years, he has studied on screening of avian flu with ICTs.



Jun-ichi Hata has received his MD degree from Keio University School of Medicine, Tokyo, in 1966. In 1971, he received a PhD degree in Keio University Post Graduate School of Medicine. Since then, he has been mainly involved in molecular pathology for pediatric tumors and embryonal pathology. He was appointed to a professor of pathology, Keio University School of Medicine in 1990. In 2013, he has been appointed as research director of Central Institute for Experimental Animals.

